Article

Journal of Industrial Textiles

2015, Vol. 45(2) 298–309

DOI: 10.1177/1528083714534710
jit.sagepub.com

Electromagnetic absorbance properties of a textile material coated using filtered arc-physical vapor deposition method

M Esen[1], I Ilhan[1], M Karaaslan[2,3], E Unal[2,3], F Dincer[3,4] and C Sabah[5]

Abstract

We explore the structure of a textile absorber in terms of its electromagnetic and absorption properties in the microwave region. Its absorption characteristics are similar to those reported for various metamaterial-based absorbers, exhibiting absorption as high as 98% at resonance. In addition, the angular behavior of the absorption properties of the sample reveal incident angle independency, which is the other added value of the study. Also, the suggested textile absorber has a simple configuration, which introduces flexibility to adjust its material properties and easily tune its structure to suit other frequencies. The proposed textile absorber and its variations have myriad potential applications in radar technology, long distance radio telecommunication, and so on. Although in its current state the proposed structure provides almost perfect absorption covering a wide range of microwave C-Band, the developing technology will soon allow manufacturing textiles that can manipulate lights, leading to the design of invisibility cloak and other science fiction devices besides finding important application areas in medical science.

[1]Vocational School of Adana, Cukurova University, Turkey
[2]Department of Electrical and Electronics Engineering, Mustafa Kemal University, Turkey
[3]Metamaterials and Photonics Research Group, Mustafa Kemal University, Turkey
[4]Department of Computer Engineering, Mustafa Kemal University, Turkey
[5]Department of Electrical and Electronics Engineering, Middle East Technical University—Northern Cyprus Campus, TRNC / Mersin 10, Turkey

Corresponding author:
C Sabah, Department of Electrical and Electronics Engineering, Middle East Technical University—Northern Cyprus Campus, Kalkanli, Guzelyurt, TRNC / Mersin 10, Turkey.
Email: sabah@metu.edu.tr

Keywords
Industrial textiles, coated fabrics, technical textile (fabric) research, engineered textiles

Introduction

Metamaterials (MTMs) have gained considerable attention in the scientific community [1–7] due to their unconventional electric and magnetic features and beneficial applications in numerous devices for different regimes of electromagnetic (EM) spectrum, from radio to optical frequencies [8–12]. These handmade artificial materials have wide potential application areas—EM cloaking [13], super lens [14], sensing [15], absorber [16,17], improvement of antenna characteristics [18], and so on [19–21]. The design and fabrication of MTMs for further and vast number of applications, either for a research purpose or at an industrial level, is highly desirable, with high yield and use of cost-effective technologies for the desired EM filtering, absorber, polarization control, sensing, or any other supplementary studies. Among the above-mentioned applications, absorbers have been one of the most studied topics and to date they continue to be investigated by the EM society [16,17]. A prototypical metamaterial absorber (MA) customarily consists of some special resonator and metallic plate separated by a dielectric substrate which is not an issue in the proposed structure anymore. In the literature, there are many studies on EM interference shielding applications including shielding based on textile materials, which describes the investigation of metal coatings and their deposition parameters on the sample [22–28]. These are generally based on some particular parameters influencing the EM shielding properties of the designed sample. Recently, many studies were performed to investigate the EM shielding properties of textile materials since the effects of EM waves emitted from electronic equipment on human health is a current problem to solve. Therefore, a number of studies were carried out to design textile-based shielding material. In order to introduce EM shielding into textile materials, various methods were used in research studies such as coating yarn using vapor phase polymerization technique [29], using metallic hybrids [30,31] or cores [32] or plied yarns [33] in fabric samples, and using composite textile materials [34]. However, there are almost no studies on use of Arc physical vapor deposition (PVD) method for imparting EM shielding properties to textile materials. In this scenario, the aim of this study is to design, realize, and experimentally analyze a perfect textile material absorber to be used in appropriate applications such as in radar technologies. Thus, we introduce and investigate a textile absorber based on Arc PVD system by adopting metallic particles on any type of surfaces for microwave C-Band. Although the main aim of the present study is to design and characterize an MTM-based textile absorber using the developing technology, the proposed method may also be used to design and realize novel types of MTMs for different applications.

It is well known that thin film coating can be realized with a thickness of a few nanometers. Different types of deposition techniques are used to meet this criterion. All of these techniques including vacuum are used to minimize unwanted

reaction with the free space and to shape the film composition easily. Two main techniques based on vacuum deposition are known as chemical vapor deposition (CVD) and PVD. In CVD technique, thin film design is realized by chemical reaction between precursors. The reaction needs hot substrate or exact deposition chamber. Due to the need of gas phase for surface coating, CVD technique is suitable for large and complex-shaped surfaces. Physical processes such as evaporation and sputtering are used in PVD technique. Some PVD methods are well known such as thermal evaporation, electron beam evaporation, and molecular beam epitaxy. Besides, many sputtering techniques are used to form plasma by collision effects of the gases in the background. All PVD methods are useful for coating surfaces faced with deposition flux. Substrate type, thin film material, necessity for uniformity, and thickness control are important parameters that help in the choice of the deposition method. In this study, cathodic arc PVD method is chosen due to its advantages over the other mentioned methods. Some of them are: materials can be co-evaporated at the same rate, better adhesion can be achieved as a result of the intermixed reaction, decent coating of heat-sensitive substrates/components, multilayered coatings, and functionally graded compositions. Because of these properties, it is preferred to be used widely in both research (as in the present study) and industrial areas to create decorative, protective, and/or wear resistant coatings without using background gases. Besides, more importantly, according to the best of our knowledge, there is no study in the literature related to the fabrication of MTMs or MTM-based devices (i.e. MTM absorber) using the cathodic arc PVD method. This may lead to design and fabrication of novel MTMs and MTM-based devices for functional components for a myriad of applications.

The absorber properties of the proposed textile absorber structure with metallic nanoparticles as textile MAs are explored and discussed in the microwave C-Band region using the reflection and transmission measurements. The coating is made of sputtered titanium nanoparticles via Arc PVD technique. There are several crucial reasons why titanium is the most appropriate metal for this type of application. First, titanium has very high temperature levels for entering into a reaction with other materials compared with the other commonly used metals. Second, Titanium is the best candidate for the health reasons. Since our structure contains fabrics, it is highly possible it comes in contact with human skin, and titanium does not cause any allergic reaction on the human body; in other words, it is health friendly. Last, titanium is lighter compared with the other commonly used metals and it has low density and high strength. Because of all these reasons, we have chosen titanium as the sputtering metal on our structure. It can precisely be fabricated without deformation over considerably large surfaces. Unlike most typical MAs, the structure does not require particular unit cell design; thus the structure provides a flexibility to design various textile MTMs, textile absorbers, and shielding structures. Besides, the structure does not suffer from the weight of the metal since it is in the form of the (nano)-particle. In general, textile structures coated with metallic nanostructures may be considered as textile MTMs since they present properties

that are similar to those of conventional MTMs. The unique properties of the textile structure also offer possible angle-independent absorbers due to their characteristic features. Besides, the proposed textile absorber has many potential advantages with respect to the conventional MA structures such as flexibility and its weight. Consequently, the suggested structure with high quality features will be a good candidate among its counterparts and can be used in radar absorbing applications. Note that, to the best of our knowledge, the present work is the first experimental study of textile MTM absorber for microwave C-band, and the data show that we succeed in achieving good absorption level for the proposed sample for the mentioned frequency range.

Materials and methods

Preparation of the sample

The samples used in this study were prepared using woven fabric. In the preparation, the sample was placed in the chamber under microfiltered cathodic arc gun. The air in the chamber was exhausted using turbomolecular pump to 3×10^{-4} to 7×10^{-4} Torr pressure, and trigger voltage was set to 20 kV and anode voltage to 550 V. Plasma arcs were applied on the material 5000–6000 times. The height of the gun from the textile surface is about 6.2 cm. The preparation was performed under room temperature conditions. The properties of the sample are given in Table 1. The fabric sample was tailored to measure 13×13 cm.

Coating of the sample

The reason for selecting the test material in fabric is to locate the nanoparticles in the material in two-dimension and non-uniformly. Figure 1 shows a typical Arc-PVD

Table 1. Properties of the textile material.

Properties of woven fabric	Values
Composition	77% cotton/33% polyamide
Weight	135 g/m^2
Weave type	3/1 S-twill
Thickness	0.25 mm
Yarn counts	Warp, spun yarn (100% cotton), Nm 70 weft, filament yarn (100% polyamide), 76 Denier
Weaving density	37 picks/cm in warp direction 67 ends/cm in weft direction
Dielectric constant	2.5–7.5 (approx.)

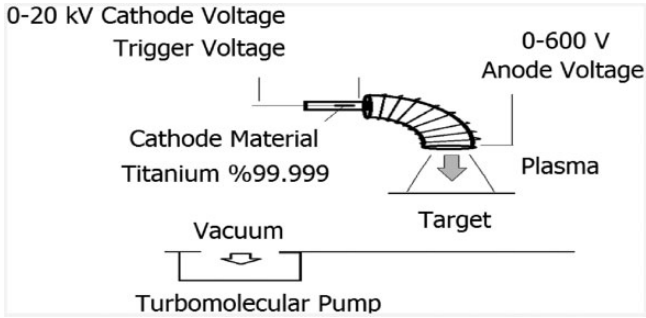

Figure 1. Arc-PVD system block diagram.
PVD: physical vapor deposition.

system block. Filtered Arc-PVD system is used to evaporate titanium metal up to 15,000°C. Consecutively, cathode spot was formed and vaporized metal nanoparticles were accelerated between 200 and 600 V and then filtered with EM toroid. The plasma thus formed is highly ionized and uncharged. Macroparticles (droplets, clusters) are filtered by 90° magnetic filter and the mentioned plasma is sputtered on textile materials. The titanium plasma sputtered on the material penetrates at various depths. The penetration depth depends on anode voltage, density of the material, and structural properties of textile materials. This method is chosen because of its various advantages. In this method, coating can be performed at room temperature, and coated surface temperature does not reach high levels; therefore, this method can be beneficial for textiles (natural and manmade) and other surfaces such as plastics, ceramic, metals, glass, and so forth, to be coated without deformation. Acceleration voltage (anode voltage) and average penetration depth can be well-controlled as required. Therefore, the adhesion of nanoparticles on most surfaces is good. The coating thickness can be controlled with the number of arc pulses, which can be considered as another advantage of the system.

Measurement of EM properties of the sample

The textile material is composed of cotton and polyamide in different ratios. Hence the effective permittivity and permeability of the uncoated-structure should be evaluated to analyze the EM properties of the proposed textile absorber. Hence the effective permittivity and permeability of the uncoated textile sample were extracted from the measured data. The measurement system is shown in Figure 2. To measure the reflection and transmission coefficients, a vector network analyzer with the range of 1–6 GHz and two horn antennas are used in this experiment [16].

Results and discussion

The extracted effective permittivity and permeability of the uncoated textile sample is shown in Figure 3. Extracted effective parameters (permittivity and permeability)

Figure 2. The test instruments used in the measurement.

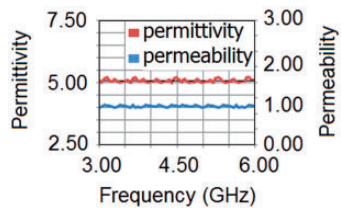

Figure 3. Extracted constitutive parameters of uncoated textile sample.

show insignificant changes with frequency (almost fixed as expected) because the uncoated sample has almost fixed constitutive parameters, as known. In addition, there is no metallic inclusion in the pure textile sample that affects and interacts with the incident wave to provide dispersive or frequency-dependent permittivity and permeability. Note that in the extraction process, the following equations are used: $\varepsilon_{eff} = n/z$ and $\mu_{eff} = n \times z$, where n is the refractive index and z is the impedance of the medium. In order to verify the existence and validity of the refractive index, a unique retrieval of effective parameters from the reflection and transmission data is obtained by enforcing the causality. The applied extraction method is based on the Kramers–Kronig (KK) relations, which have been used to calculate the index of refraction using calculated or measured data sets [35]. While the real part of the complex refractive index has multiple solutions, the imaginary part of the refractive index is not affected by the branch problem of the standard retrieval method. Thus, the imaginary part has a unique solution and it can be calculated without ambiguity. By knowing the unique imaginary part of the refractive index, the real part can be determined using KK relations and the

guidance of the imaginary part for the correct choice of the branch. The KK relation for the real part of the refractive index can be written as follows

$$Re\{n_{eff}(f)\} = 1 + \frac{2}{\pi} P \int_0^{\infty} \frac{f' Im\{n_{eff}(f')\}}{f'^2 - f^2} df' \quad (1)$$

where P designates the principal value of the integral. Note that to compute the given integral accurately, the imaginary part of the refractive index must be known for the entire spectrum. For practical reasons, the given integral has to be truncated, which yields some error. Nevertheless, the evaluation of KK equation (equation (1)) even for the finite bandwidth can provide approximate data for the verification of the actual data. For details, one can see the study of Sabah and Roskos [35]. The figure has two axes in which the left scale represents the effective permittivity while the right scale refers to the effective permeability of the uncoated sample. The extracted relative permittivity of the sample is around 5.0, which is in the estimated range shown in Table 1. The extracted permeability was around 1.0, as expected. The extracted permittivity and permeability values of the sample are almost constant for the studied frequency region as expected, and they are in good agreement with the literature [36–38]. The extracted values depend on the properties, materials used, and the composition of the sample (which are already defined in Table 1).

Moreover, views of the textile material and Arc-PVD processed textile material using scanning electron microscopy (SEM) are shown in Figure 4. SEM generates images of any sample by scanning it with a focused beam of electrons. The electrons interact with atoms in the sample, generating various EM signals. These signals can be detected and contain information about the surface topography and the composition of the sample. Scanning generators supply necessary voltages or currents for the deflection circuits of the microscope and of the display. The ratio of these deflections gives, of course, the magnification of the instrument. The pictures are magnified with a ratio of $\times 100$ (Figure 4(a) and (b)) and $\times 1000$ (Figure 4(c) and (d)). Evidently, the yarns coated with titanium nanometals are brighter (Figure 4(b) and (d)) than the uncoated ones (Figure 4(a) and (c)). The metallic surfaces on yarn and metallic ground plane will have both electric and magnetic responses to provide a resonance within the studied frequency region. In this case, the impedance of the textile material will be matched with the free space impedance at the resonance frequency. Hence, incident wave can penetrate the material abundantly.

For the perfect absorption, the transmission and reflection coefficients of incident waves have to be nearly zero($R(\omega)$ &$T(\omega) \rightarrow 0$). In general, the absorption level is obtained using $A(\omega) = 1 - R(\omega) - T(\omega)$, where $A(\omega)$, $R(\omega) = |S_{11}|^2$, and $T(\omega) = |S_{21}|^2$ represent the absorption, reflection, and transmission, respectively. To realize an abundant absorption at a certain frequency range, the reflection and transmission coefficients should be minimized by matching the impedances (the effective impedance of the medium to the free space impedance $Z(\omega) = Z_0(\omega)$) [16].

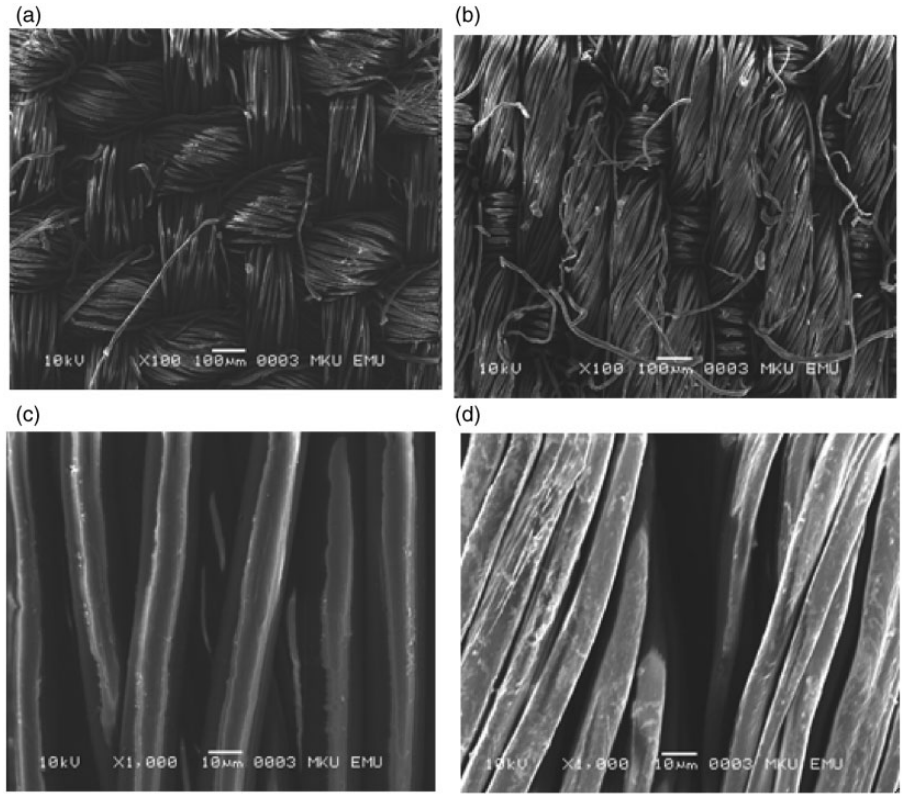

Figure 4. SEM images of the textile samples, (a) and (c) uncoated and (b) and (d) coated, with metal using Arc-PVD method.
SEM: scanning electron microscopy.

The transmission, S_{21}, will be zero in the proposed absorber due to the metallic background of the sample. Therefore, only the measured reflection S_{11} and absorption results are presented in Figure 5. The resonance appeared at 4.42 GHz with $S_{11} = 0.08$. Experimentally, the maximum value in the absorption was obtained around 98% at resonance. The reflection and absorption values are very significant for such samples in the microwave region. There is also absorption of 0.75 at 5.20 GHz, but this peak value does not match with standard absorption values.

It is a well known fact that there are many factors that affect the resonance frequencies such as effective permittivity, effective permeability, loss tangent, thickness of textile sample, surface density of coating metal, and so on. For example, maximum absorption is observed in the case of equivalent impedance values of free space and overall textile sample composed of coated surface, pure textile material, and metallic ground plane. While the free space impedance is $Z(\omega) = Z_0(\omega) = 120\pi$, the intrinsic impedance of the textile sample is

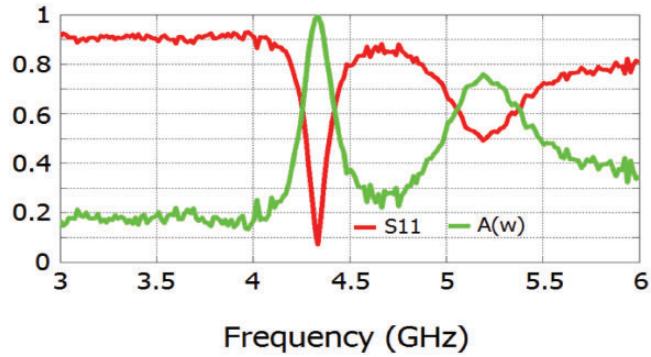

Figure 5. Reflection and absorption coefficient of the sample.

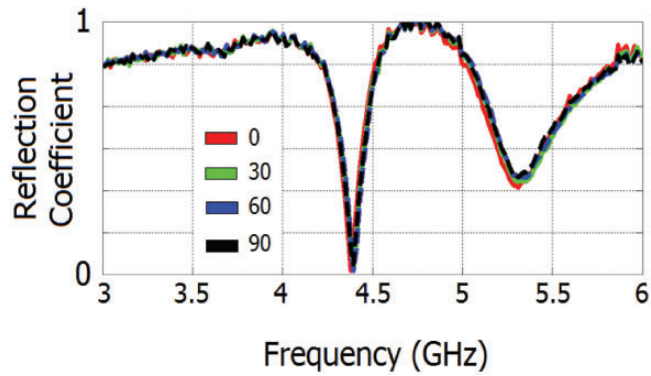

Figure 6. Reflection coefficient of the sample for different incident angles.

$Z(\omega) = \sqrt{\mu(\omega)/\varepsilon(\omega)}$. If the effective dielectric constant of textile sample, $\varepsilon(\omega)$, decreases, the intrinsic impedance of the textile sample will increase and the resonance frequency shifts upward or downward until the intrinsic and free space impedance are equal.

Next, the incident angle is changed to understand the angular properties of the proposed absorber. Figure 6 shows the reflection coefficient versus frequency under different incident angles. Reflection coefficient does not change with respect to the variation of the incident angle, meaning that the textile absorber also is independent of the incident angle, which can be used in many applications.

The proposed textile absorber is incident angle independent since the Arc PVD metallization for coating is homogenously deposited on the textile sample and the metallization does not exhibit axial dependency, as shown in SEM images (Figure 4). Hence, change of the incident wave angle does not affect current distribution of the homogenized metallic inclusions.

Conclusion

In conclusion, the proposed textile absorber was introduced and experimentally investigated for microwave C-Band frequency region. The results obtained show that the model can be used as a perfect absorber with incident angle independency. In addition to that, it is also suitable for myriad absorber applications due to its flexibility of design. To the best of our knowledge, this is the first study on such a textile absorber that is independent of the incident angle. Since the structure provides a resonance at the microwave C-Band frequency region and offers perfect absorption with independence from the incident angle at the mentioned regime, it can also be used in long-distance radio telecommunications (as directly related with C-Band), and it will be a very good candidate in the application of satellite communications transmissions, Wi-Fi devices, cordless telephones, weather radar systems, and so on. Moreover, the proposed model can be retailored for different frequencies to be used in different applications.

Funding

MK acknowledges the support of TUBITAK (project number 113E290) and partial support of the Turkish Academy of Sciences.

References

[1] Hashsish EA. Design of wideband thin layer planar absorber. *J Electromagn Waves Appl* 2002; 16: 227–241.
[2] Sabah C, Tastan HT, Dincer F, et al. Transmission tunneling through the multilayer double-negative and double-positive slabs. *Prog Electromagn Res* 2013; 138: 293–306.
[3] Sabah C and Roskos HG. Design of a terahertz polarization rotator based on a periodic sequence of chiral metamaterial and dielectric slabs. *Prog Electromagn Res* 2012; 124: 301–314.
[4] Dincer F, Sabah C, Karaaslan M, et al. Asymmetric transmission of linearly polarized waves and dynamically wave rotation using chiral metamaterial. *Prog Electromagn Res* 2013; 140: 227–239.
[5] Guo XR, Zhang Z, Wang JH, et al. The design of a triple-band wide-angle metamaterial absorber based on regular pentagon close-ring. *J Electromagn Waves Appl* 2013; 27: 629–637.
[6] Zarifi D, Soleimani M and Nayyeri VA. Novel dual-band chiral metamaterial structure with giant optical activity and negative refractive index. *J Electromagn Waves Appl* 2012; 26: 251–263.
[7] Sabah C. Multiband metamaterials based on multiple concentric open-ring resonators topology. *IEEE J Sel Top Quant* 2013; 19: 8500808.
[8] Smith DR, Padilla WJ, Vier DC, et al. Composite medium with simultaneously negative permeability and permittivity. *Phys Rev Lett* 2000; 84: 4184–4187.
[9] Yen TJ, Padilla WJ, Fang N, et al. Terahertz magnetic response from artificial materials. *Science* 2004; 303: 1494–1496.

[10] Linden S, Enkrich C, Wegener M, et al. Magnetic response of metamaterials at 100 terahertz. *Science* 2004; 306: 1351–1353.
[11] Zhang S, Fan W, Panoiu NC, et al. Experimental demonstration of near-infrared negative-index metamaterials. *Phys Rev Lett* 2005; 95: 137404–4.
[12] Dolling G, Wegener M, Soukoulis CM, et al. Negative-index metamaterial at 780 nm wavelength. *Opt Lett* 2007; 32: 53–55.
[13] Song W and Sheng XQ. A cloak scheme insusceptible to the change of material properties. *J Electromagn Waves Appl* 2012; 26: 149–160.
[14] Zhang Y and Fiddy MA. Covered image of superlens. *Prog Electromagn Res* 2013; 136: 225–238.
[15] Cai M and Li EP. A novel terahertz sensing device comprising of a parabolic reflective surface and a bi-conical structure. *Prog Electromagn Res* 2009; 97: 61–73.
[16] Dincer F, Karaaslan M, Unal E, et al. Dual-band polarization independent metamaterial absorber based on omega resonator and octa-star strip configuration. *Prog Electromagn Res* 2013; 141: 219–231.
[17] Sun J, Liu L, Dong G, et al. An extremely broad band metamaterial absorber based on destructive interference. *Opt Express* 2011; 19: 21155–21162.
[18] Li D, Szabó Z, Qing X, et al. A high gain antenna with an optimized metamaterial inspired superstrate. *IEEE Trans Ant Propag* 2012; 60–12: 6018–6023.
[19] Rezvani S, Atlasbaf Z and Forooraghi KA. Novel miniaturized reconfigurable slotted microstrip patch antenna with defected ground structure. *J Electromagn Waves Appl* 2011; 31: 349–354.
[20] Shoukat S, Ahmed S, Ashraf MA, et al. Scattering of electromagnetic plane wave from a chiral cylinder placed in chiral metamaterials. *J Electromagn Waves Appl* 2013; 27: 1127–1135.
[21] Yilmaz A and Sabah C. Diamond-shaped hole array in double-layer metal sheets for negative index of refraction. *J Electromagn Waves Appl* 2013; 27: 413–420.
[22] Tennant A, Hurley W and Dias T. Experimental knitted, textile frequency selective surfaces. *Electron Lett* 2012; 48: 1386–1388.
[23] Roh JS, Chi YS, Kang TJ, et al. Electromagnetic shielding effectiveness of multifunctional metal composite fabrics. *Text Res J* 2008; 78: 825–835.
[24] Wieckowski TW and Janukiewicz JM. Methods for evaluating the shielding effectiveness of textiles. *Fibres Text East Eur* 2006; 14: 18–22.
[25] Pande S, Singh BP, Mathur RB, et al. Improved electromagnetic interference shielding properties of MWCNT-PMMA composites using layered structures. *Nanoscale Res Lett* 2009; 4: 327–334.
[26] Bingqing Y, Liming Y, Leimei S, et al. Comparison of electromagnetic interference shielding properties between single-wall carbon nanotube and graphene sheet/polyaniline composites. *J Phys D: Appl Phys* 2012; 45(23): 235108.1–235108.6.
[27] Ramôa SD, Barra GM, Oliveira RV, et al. Electrical, rheological and electromagnetic interference shielding properties of thermoplastic polyurethane/carbon nanotube composites. *Polym Int* 2013; 62: 1477–1484.
[28] Savitha Kadencheri Unnikrishnan, Vinayasree S, Gurumallesh Prabu Halliah, et al. Flexible electromagnetic interference shields in S band region from textile materials. *J Ind Text* 2013; 43(2): 215–230.

[29] Yildiz Z, Usta I and Gungor A. Investigation of the electrical properties and electromagnetic shielding effectiveness of polypyrrole coated cotton yarns. *Fibres Text East Eur* 2013; 21: 32–37.
[30] Ortlek HG, Alpyildiz T and Kilic G. Determination of electromagnetic shielding performance of hybrid yarn knitted fabrics with anechoic chamber method. *Text Res J* 2013; 1: 90–99.
[31] Grabowska KE, Marciniak K and Ciesielska-Wróbel IL. The analysis of attenuation of electromagnetic field by woven structures based on hybrid fancy. *Text Res J* 2011; 81: 1578–1593.
[32] Duran D and Kadoglu H. A research on electromagnetic shielding with copper core yarns. *J Text Apparel* 2012; 22: 354–359.
[33] Perumalraj R and Dasaradan BS. Electromagnetic shielding effectiveness of doubled copper-cotton yarn woven materials. *Fibres Text East Eur* 2010; 18: 74–80.
[34] Chen HC, Lee KC and Lin JH. Electromagnetic and electrostatic shielding properties of co-weaving-knitting fabrics reinforced composites. *Compos Part A: Appl Sci* 2004; 35: 1249–1256.
[35] Sabah C and Roskos HG. Dual-band polarization-independent sub-terahertz fishnet metamaterial. *Curr Appl Phys* 2012; 12: 443–450.
[36] Declercq F, Rogier H and Hertleer C. Permittivity and loss tangent characterization for garment antennas based on a new matrix-pencil two-line method. *IEEE Trans Ant Propag* 2008; 56-8: 2548–2554.
[37] Ren Y and David CC Lam. Properties and microstructures of low-temperature-processable ultralow-dielectric porous polyimide films. *J Electronic Mater* 2008; 37(7): 955–961.
[38] Salvado R, Loss C, Goncalves R, et al. Textile materials for the design of wearable antennas: A survey. *Sensors* 2012; 12(11): 15841–15857.